FULL-LENGTH ORIGINAL RESEARCH

White matter abnormalities associate with type and localization of focal epileptogenic lesions

***Brunno M. Campos, *Ana C. Coan, †Guilherme C. Beltramini, ‡Min Liu, *Clarissa L. Yassuda, *Enrico Ghizoni, ‡Christian Beaulieu, §Donald W. Gross, and *Fernando Cendes**

Epilepsia, 56(1):125–132, 2015
doi: 10.1111/epi.12871

Brunno M. Campos is a doctoral student at the University of Campinas.

Summary

Objective: **To evaluate white matter (WM) integrity of distinct groups of patients with antiepileptic drug (AED)–resistant localization-related epilepsies.**

Methods: **We used diffusion tensor imaging (DTI) fiber-tractography and voxel-based morphometry (VBM) to investigate differences of WM micro- and macrostructural integrity in patients with different drug-resistant localization-related epilepsies: 17 with temporal lobe epilepsy with magnetic resonance imaging (MRI) signs of hippocampal sclerosis (TLE-HS), 17 with TLE and normal MRI (TLE-NL), 14 with frontal lobe epilepsy and subtle MRI signs of focal cortical dysplasia (FLE-FCD), and 112 healthy controls. We performed fiber-tractography using a semiautomatic deterministic method to yield average fractional anisotropy (FA), axial (AD), and radial (RD) diffusivity ipsilateral and contralateral to the epileptogenic zone of the following tracts based on their functional and anatomic relevance: body of fornix (BoF), body of cingulum (BoC), inferior frontal occipital (IFO), and uncinate fasciculi (UF). In addition, we performed VBM of the WM maps to assess macrostructural integrity differences among groups.**

Results: **TLE-HS had ipsilateral and contralateral decreased FA and increased RD for all tracts. VBM showed WM alterations mainly in the ipsilateral parahippocampal region and contralateral superior temporal gyrus. FLE-FCD showed bilateral FA decreases only in the BoC and ipsilateral RD increases also in the BoC. VBM showed WM reduction mainly in the ipsilateral precuneus and posterior and anterior cingulum. No significant WM alterations were found in the TLE-NL in DTI or VBM analysis.**

Significance: **WM abnormalities differ in distinct AED-resistant localization-related epilepsies. The diverse distribution of the WM damage in these patients suggests that the localization of the epileptic networks may play a role in the WM burden. However, the distinct degree of this damage, more accentuated in TLE-HS, also suggests that the underlying cause of the epilepsy is probably an additional factor to explain this WM damage.**

KEY WORDS: **Frontal lobe epilepsy, Temporal lobe epilepsy, Diffusion tensor imaging, Voxel-based morphometry.**

Accepted October 14, 2014; Early View publication December 26, 2014.

*Neuroimaging Laboratory, Department of Neurology, University of Campinas, Campinas, Brazil; †Neurophysics Group, Gleb Wataghin Physics Institute, University of Campinas, Campinas, Brazil; ‡Department of Biomedical Engineering, Faculty of Medicine and Dentistry, University of Alberta, Edmonton, Alberta, Canada; and §Division of Neurology, Department of Medicine, Faculty of Medicine and Dentistry, University of Alberta, Edmonton, Alberta, Canada

Address correspondence to Fernando Cendes, Departamento de Neurologia, Faculdade de Ciências Médicas – UNICAMP, Cidade Universitária Zeferino Vaz, Campinas SP CEP 13083-970, Brazil. E-mail: fcendes@unicamp.br

Structural neuroimaging studies have shown ample evidence that antiepileptic drug (AED)–resistant epilepsies, especially temporal lobe epilepsy (TLE) with hippocampal sclerosis (HS), have widespread gray matter abnormalities extending beyond the epileptogenic zone.[1,2] Moreover, widespread white matter (WM) density abnormalities have also been observed in these patients.[1,3] Previous diffusion tensor imaging (DTI) tractography studies reported abnormal WM tracts in various epilepsies.[4–7] In TLE-HS, DTI studies show bilateral and diffuse abnormal integrity, whereas in TLE with normal routine magnetic resonance imaging (MRI), the WM abnormalities are subtler.[8–13] These findings are concordant with the results of voxel-based morphometry (VBM) studies.[1,2] DTI can also delineate focal WM lesions in patients with focal cortical dysplasia (FCD), and may help explain the ictal spreading.[8,14,15.]

So far the causes or the consequences of these WM abnormalities have not been well clarified. Although cross-sectional studies will not definitively solve this question, the comparison of the patterns of WM abnormalities in different epileptic syndromes can improve our knowledge about the possible causes of WM damage. The purpose of the present study was to use VBM to look for macrostructural WM abnormalities, and DTI analysis to provide inferences of the WM microstructure for the evaluation of three distinct types of AED-resistant localization-related epilepsies: (1) TLE associated with HS (TLE-HS); (2) TLE with normal MRI (TLE-NL); and (3) frontal lobe epilepsy with subtle MRI abnormalities suggestive of focal cortical dysplasia (FLE-FCD). We hypothesized that WM damage occurs in AED-resistant localization-related epilepsies irrespective of the epileptic syndrome, and that the pattern of WM damage is different according to the localization of the presumed epileptogenic zone and the etiology.

Methods

Subjects

All patients and controls included in this study signed informed consent, approved by the ethics committee of the Faculty of Medical Sciences of the University of Campinas.

We included 48 patients with AED-resistant localization-related epilepsy followed at the Epilepsy Center of University of Campinas who fulfilled the inclusion criteria described later. The patients were selected according to one of the following characteristics:

1 TLE-HS: Clinical and electroencephalography (EEG) characteristics of TLE and MRI signs of HS (Fig. 1A). There were 17 patients with mean age of 38 years (age range 26–60 years; 77% women). Five of these patients underwent surgical resection due to refractory seizures with HS confirmed by histopathology and all have Engel class Ia surgical outcome after an average follow-up of 30 months;
2 TLE-NL: Clinical and EEG characteristics of TLE and normal routine MRI (Fig. 1B). There were 17 patients with mean age of 37 years (age range 21–61 years; 65% women). One patient underwent surgery due to refractory seizures with nonspecific findings revealed by histopathology and this patient has Engel class Ia surgical outcome after a follow-up of 27 months;
3 FLE-FCD: Clinical and EEG characteristics of FLE and subtle MRI abnormalities suggestive of FCD (Fig. 1C). There were 14 patients with mean age of 33 years (age range 22–49 years; 64% women). Two of these patients underwent surgical resection due to refractory seizures with FCD type IIA confirmed by histopathology,[16] and all had Engel class III surgical outcome after an average follow-up of 24 months. The maintenance of seizures in these patients was attributed to the incomplete resection of the FCD because of the proximity of eloquent cortex.

Only patients with a clearly defined epileptogenic zone were selected (see Supporting Information, Table S1, for details). The epileptogenic zone of each patient was defined by a panel of specialists based on an extensive workup, which included prolonged scalp EEG recordings (average of 200 min), video-EEG and, when appropriate, Fluorodeoxyglucose–positron emission tomography (PET) or ictal single photon emission computed tomography (SPECT). All TLE-HS and FLE-FCD patients had the localization of the epileptogenic zone concordant with the MRI abnormality.

After a visual analysis for quality control of the MRI images, we included a group of 112 healthy individuals

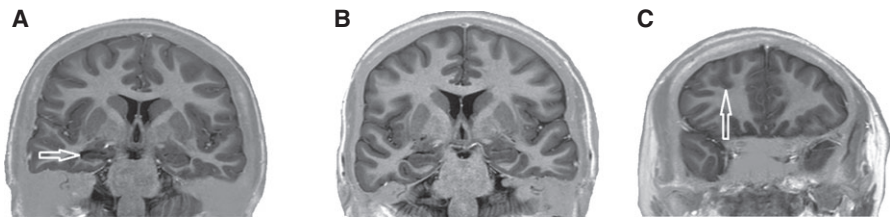

Figure 1.
Example of coronal inverse recovery images of patient groups. (**A**) TLE-HS: arrow shows reduced right hippocampal volume compatible with hippocampal sclerosis; (**B**) TLE-NL: no MRI abnormalities detected; (**C**) FLE-FCD: arrow shows deep abnormal sulcus suggestive of focal cortical dysplasia.

(mean age 35 years; age range 20–60 years; 68% women) for comparisons in the DTI study and a subset of 72 healthy individuals (mean age 32 years; age range 21–61 years; 56% women) for VBM analysis. Controls subjects were excluded from the VBM analysis because of image movement artifacts or different acquisition parameters. In this study, we acquired all MRI data on a 3T Philips Achieva (Best, The Netherlands) at the Neuroimaging Laboratory, University of Campinas- UNICAMP, Campinas, São Paulo, Brazil.

We defined MRI signs of HS as reduced volume and loss of internal structure of hippocampus on coronal T_1-weighted images acquired perpendicular to the long axis of hippocampus (T_1"inversion recovery", 3 mm thick, no gap, voxel size = 0.75 × 0.75 × 3 mm^3, repetition time (TR) = 3,550 msec, echo time (TE) = 15 msec, inversion time = 400 msec, matrix = 240 × 229, field of view [FOV] = 180 × 180 mm^2, Turbo Spin Echo [TSE] factor = 7) and hippocampal signal hyperintensity on T_2-weighted and fluid-attenuated inversion recovery (FLAIR) images (coronal T_2 multi-echo image: 3 mm thick, no gap, voxel size = 0.89 × 1 × 3 mm^3, TR = 3,300 msec, TE = 30/60/90/120/150 msec, matrix = 200 × 180, FOV = 180 × 180 mm^2, TSE factor = 5; echo planar imaging (EPI) factor = 5; flip angle = 90 degrees; FLAIR coronal and axial images: 4 mm thick, slice gap = 1 mm, voxel size = 0.89 × 1.12.4 mm^3, TR = 12,000 msec, TE = 140 msec, inversion time = 2,850 msec, matrix = 180 × 440, FOV = 200 × 200 mm^2). The presence or absence of MRI signs of HS was also confirmed by automated volumetry and manual T_2 signal quantification.[17]

We defined MRI signs of FCD as an area of cortical thickening, loss of the sharp interface between white and gray matter, and focal atrophy with or without T_2 hyperintense signal.[16,18] We did not observe transmantle signs in any of these exams. For the patients classified as FLE-FCD, the MRI exams were initially considered normal and the abnormalities were observed after multiplanar reconstruction of T_1 and T_2 images (T_1W with isotropic voxels of 1 mm, acquired in the sagittal plane, 1 mm thick, no gap, flip angle = 8 degrees, TR = 7.0 msec, TE = 3.2 msec, matrix = 240 × 240, FOV = 240 × 240 mm^2; T_2W with isotropic voxels of 1.5 mm, acquired in the sagittal plane, no gap, TR = 1,800 msec, TE = 340 msec, matrix = 140 × 140, FOV = 230 × 230 mm^2, TSE factor = 120; flip angle = 90 degrees; geometry corrected).[18] In addition, we carefully evaluated the MRI images of patients in the TLE-NL group with multiplanar reconstruction, and selected only those without signs suggestive of FCD.

DTI analysis

DTI analysis provides inferences of the WM microstructure noninvasively by measuring the anisotropic water diffusion of the axon tracts. The basic assumption in DTI measurements is that the water diffusion perpendicular to the fiber orientation is constrained by axon membranes and myelination, whereas it is less hindered along the tract.[19,20] In this sense, the measures of fractional anisotropy (FA) and diffusion values as axial diffusivity (AD) or diffusivity in the tract direction, and radial diffusivity (RD) or diffusivity perpendicular to the tract direction, can quantify and characterize the water molecules movement, allowing an indirect assessment of the tract "integrity." DTI tractography also allows the virtual reconstruction of the WM tracts. It provides in vivo depiction of large fasciculi and increases the specificity through the definition of pathology-relevant anatomic regions.[21]

For tractography analysis, we acquired a spin-echo single-shot echo planar imaging (EPI) (2 × 2 × 2 mm^3 acquiring voxel size, interpolated to 1 × 1 × 2 mm^3; reconstructed matrix 256 × 256; 70 slices; TE/TR 61/8,500 msec; flip angle 90 degrees; 32 gradient directions; no averages; max b-factor = 1,000 s/mm^2; 6-min scan).

We chose four tracts based on their functional and anatomic relevance to the spread of focal seizures originating in the temporal and frontal lobes: (1) body of the cingulum (BoC); (2) body of the fornix (BoF); (3) uncinate fasciculi (UF); and (4) inferior frontooccipital (IFO) fasciculi (Fig. 2). The tensor calculation of all images was performed using the ExploreDTI software (A. Leemans, University Medical Center, Utrecht, The Netherlands) and the fiber tractography through a semiautomatic deterministic methodology briefly described later.[22] Regions of interest (ROIs) to seed each tract were manually drawn on a normalized

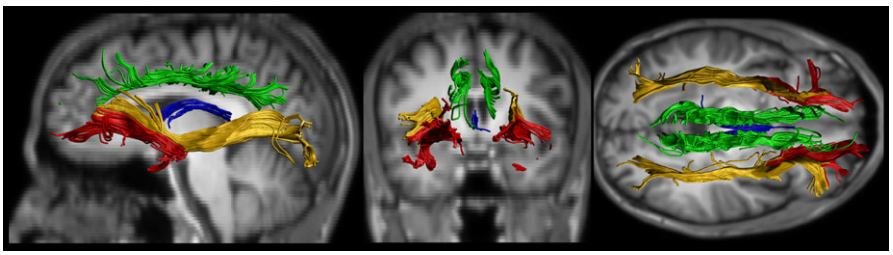

Figure 2.
Fiber tractography of the studied tracts in a control subject. In green, the body of cingulum (BoC); in blue, the body of fornix (BoF); in red, the uncinate fasciculi (UF); in yellow, the inferior frontooccipital fasciculi (IFO).

template. In this study, this template was created with non–diffusion-weighted images of 10 local control subjects (mean age 33 years; age range 22–47 years; 50% women) acquired in the same MRI scanner, aiming to improve the anatomic matching to the study sample. Sequentially, the method uses the three-dimensional (3D) deformation field matrix of each subject to apply an inverse normalization operation (Statistical Parametric Mapping 8 [SPM 8]-deformation fields algorithm), using the variants between native and standardized space to bring the normalized ROIs to that subject-specific space. Finally, the adjusted (native space) ROIs were used for the fiber tracking.

The fiber-tracking parameters set were the same for all studied fasciculi: minimal FA to start tract 0.25; minimal FA to keep tracking 0.25; maximal tract angle 60°; and minimal fiber length 10 mm. We visually checked the resultant tracts and separately calculated the average FA, AD, and RD for each hemisphere. The diffusion values were estimated by averaging all voxels in a given tract.

FA, AD, and RD values were lateralized as ipsilateral or contralateral to the presumed epileptogenic zone as defined by ictal/interictal scalp EEG recordings and concordant lateralized MRI abnormality (due to its interhemispheric positioning, the BoF will be always described without lateralization). The control subjects had their laterality defined randomly with the same proportions of patient groups (37% of the group within the right hemisphere considered as ipsilateral) and the gender ratio. The statistical analyses were performed using SPSS version 20 (IBM SPSS Statistics for Windows, Version 20. IBM Corp., Armonk, NY, U.S.A.). Multivariate General Linear Model (mGLM) with Tukey's honestly significant difference post hoc test was used to evaluate differences between groups. Three distinct mGLM were performed, comparing FA, AD, and RD separately, whereas in each model, the ipsilateral and contralateral average values of each tract were included. Each mGLM post hoc test gave corrected (for multiple comparisons) p-values, and also these statistical results were additionally controlled by the false discovery rate (FDR) accounting for the three independent comparisons.

VBM analysis

For the VBM analysis, we used VBM8 plus DARTEL toolbox (http://dbm.neuro.uni-jena.de/vbm/). All T_1-weighted images were preprocessed using SPM8/VBM8 routines. The images were spatially normalized to the same stereotaxic space (A Fast Diffeomorphic Registration Algorithm [DARTEL] algorithm, MNI- Montreal Neurological Institute - 152), segmented into WM, gray matter, and cerebrospinal fluid, modulated (aiming to correct to local volume changes during the normalization) and smoothed with an isotropic Gaussian kernel of 10 mm. The postprocessed WM image homogeneity was checked and finally compared using a voxel-wise statistical analysis. All patients with the epileptogenic zone on the right side had their images lateralized to the left side, so in the following section the left side is referred to as ipsilateral and the right as contralateral to the epileptogenic zone. The control images were randomly flipped in the same proportions (37%). The analysis of covariance (ANCOVA) test was performed to compare the groups of controls and patients using age and gender as covariates. Three different contrasts were designed to separately verify the WM atrophy in each group of patient (family wise error (FWE) correction with $p < 0.05$ and minimum cluster size of five contiguous voxels).

Results

Multivariate analyses of variance (MANOVAs) tested the similarity between the three groups of patients. There were no significant differences of the distribution of age ($p = 0.39$; mean 35 years; range 60–21 years), gender ($p = 0.70$), and epilepsy duration ($p = 0.09$; mean 22 years; range 53–22 years). MANOVA showed significant difference for age of seizure onset, with TLE-NL having older mean age at onset ($p = 0.01$; Table 1). No difference in age (MANOVA p-value = 0.677; mean 35 years; range 60–20 years) and gender (MANOVA $p = 0.788$) distribution was observed between the three groups of patients and controls. Additional clinical data are summarized in Table 1.

DTI analysis

The mGLM performed to test FA between controls and the three epilepsy groups showed significant decrease of FA ipsilateral to the epileptogenic zone for the BoC ($p < 0.001$), IFO ($p < 0.001$), and UF ($p < 0.001$). There was also decreased FA for the BoF ($p = 0.003$). The Tukey's post hoc pairwise comparisons revealed significant FA decrease for the TLE-HS for all ipsilateral fasciculi (BoC $p = 0.003$; IFO $p < 0.001$; UF $p < 0.001$) and for the BoF ($p = 0.002$). Compared to controls, FLE-FCD group showed significant FA decreases in the post hoc test only in the BoC ($p = 0.011$).

On the contralateral side, mGLM showed significant FA decreases for BoC ($p < 0.001$), IFO ($p < 0.001$), and UF

Table 1. Clinical data and demography

	TLE-HS	TLE-NL	FLE-FCD
Gender	4 male/13 female	6 male/11 female	5 male/9 female
Age	38 (26–59) years	36 (21–60) years	33 (21–48) years
First seizure	9 (0.2–17) years	16 (2–45) years	7 (1–14) years
Epilepsy duration	28 (11–52) years	20 (4–39) years	25 (11–46) years
Family history	6 (35%)	8 (47%)	3 (21.4%)
Laterality (EZ)	5 right/12 left	3 right/14 left	10 right/4 left
SGTCS[a]	1 (5%)	3 (17%)	7 (50%)

[a]History of SGTCS in Past year.

EZ, Epileptogenic zone; IPI, initial precipitating injuries; TLE-HS, temporal lobe epilepsy with hippocampal sclerosis; TLE-NL, nonlesional temporal lobe epilepsy; FLE-FCD, frontal lobe epilepsy-focal cortical dysplasia; SGTCS, secondary generalized tonic–clonic seizure.

($p = 0.006$). The Tukey's post hoc pairwise comparisons revealed significant FA differences between controls and TLE-HS in all contralateral fasciculi (BoC $p = 0.001$; IFO $p < 0.001$; UF $p = 0.007$). Compared to controls, the FLE-FCD group showed contralateral significantly decreased FA only in the BoC ($p = 0.048$).

We found no significant differences between controls and TLE-NL. The average ipsilateral FA values for each tract of all groups with the respective standard deviations are shown in Figure 3A.

There were no significant differences of AD in the ipsi- and contralateral fasciculi or the BoF for each epilepsy group versus controls. The average ipsilateral AD values of each tract with respective standard deviations are represented in Figure 3B.

There were significant ipsilateral alterations of RD in all studied tracts: BoC ($p < 0.001$), IFO ($p = 0.001$) and UF ($p < 0.001$) as well as the BoF ($p = 0.031$). The post hoc pairwise comparisons showed RD differences between controls and TLE-HS in the ipsilateral BoC ($p = 0.004$), IFO ($p = 0.001$), and UF ($p < 0.001$), and also in the BoF ($p = 0.027$). Furthermore, the post hoc test showed ipsilateral decrease of RD in FLE-FCD compared to controls only for the BoC ($p = 0.022$). No significant differences for ipsilateral RD values were found comparing controls and TLE-NL.

There was also differences of RD in the contralateral side for all studied tracts (BoC $p < 0.001$, IFO $p = 0.001$, and UF $p = 0.006$). The Tukey's post hoc pairwise comparisons revealed significant increases of the RD values on the contralateral side only for the TLE-HS group compared to controls (BoC $p = 0.003$, IFO $p = 0.001$, and UF $p = 0.003$).

VBM analysis

In comparison with controls, TLE-HS showed extensive mesial temporal WM volumetric decreases including mesial temporal regions, thalamic region, and posterior cingulum in the hemisphere ipsilateral to the epileptogenic zone but also in the superior temporal gyrus contralateral to the epileptogenic zone (Fig. 4A). For the FLE-FCD group, VBM showed significant WM atrophy exclusively localized in the hemisphere ipsilateral to the epileptogenic zone including the anterior and posterior cingulum and precuneus (Fig. 4C). No WM volumetric alterations were found in the TLE-NL group (Fig. 4B). All complementary results are presented in Table 2.

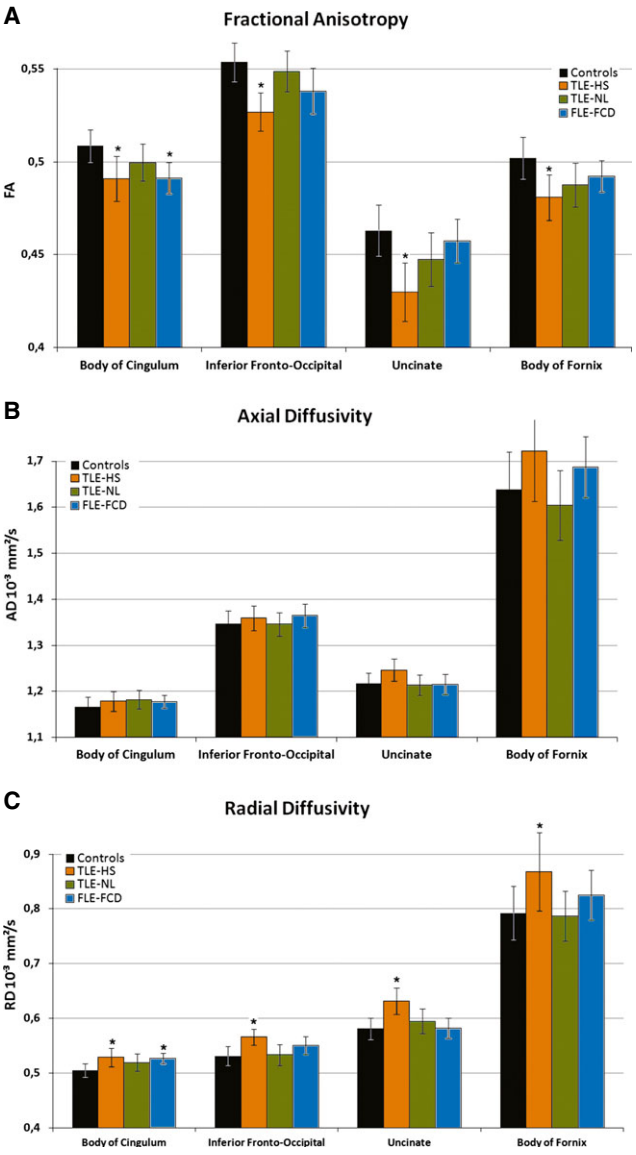

Figure 3.
Ipsilateral average diffusion values (and BoF total diffusion values) separated by tracts and groups. TLE-HS patients presented decreased FA (**A**) and increased radial diffusivity (**C**) for all tracts, while FLE-FCD patients showed decreased FA and increased RD only in the BoC. No abnormalities in axial diffusivity (**B**) were found in this study. TLE-NL patients did not have diffusion abnormalities in any of these tracts. The * indicates parameters with significant difference (mGLM, Tukey's post hoc test, $p < 0.05$) when compared to control group.

Discussion

In the current study, WM micro- and macrostructural integrity was evaluated in three groups of AED-resistant localization-related epilepsies. Our results demonstrate that the patterns and the degree of WM abnormalities differ among groups according to the localization of the epileptogenic zone and the presumed etiology. Although patients with TLE-HS are those with the most diffuse injury, WM damage also occurs in FLE-FCD but could not be detected in TLE-NL by either DTI or VBM.

In this study, both DTI and VBM showed that patients with TLE-HS have widespread abnormalities in tract integrity including extratemporal structures such as cingulum.[11,23,24] Although extratemporal areas in both

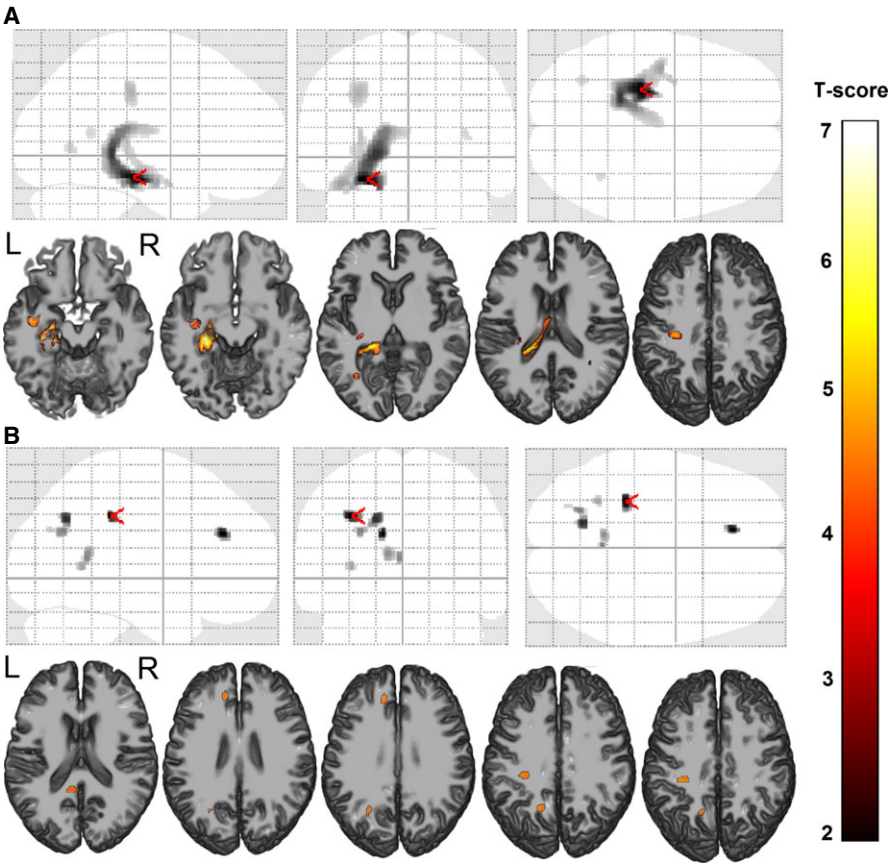

Figure 4.
White matter (WM) voxel-based morphometry results ($p < 0.05$ FWE corrected, cluster with at least five voxels). (**A**) Temporal lobe epilepsy associated with hippocampus sclerosis: extensive WM atrophy in the ipsilateral parahippocampal gyrus (global maxima). (**B**) Frontal lobe epilepsy with MRI signs of focal cortical dysplasia: WM atrophy restricted to the ipsilateral hemisphere and more important in the post central gyrus. Red arrow heads indicate the most statistically significant areas. Temporal lobe epilepsy with normal MRI presented no WM atrophy using this statistical threshold.
Epilepsia © ILAE

Table 2. White matter voxel-based morphometry of T_1-weighted MRI

Group	Laterality	Coordinate	N° Voxels	Structure
TLE-HS	Ipsi	−26 −24 −15	1,294	Parahippocampal gyrus
	Ipsi	−30 −25 42	212	Postcentral gyrus
	Ipsi	−33 −63 4	30	Middle occipital gyrus
	Contra	36 −51 13	15	Superior temporal gyrus
TLE-NL	–	–	–	–
FLE-FCD	Ipsi	−32 −33 39	64	Postcentral gyrus
	Ipsi	−12 38 28	46	Medial frontal gyrus
	Ipsi	17 −63 37	86	Precuneus
	Ipsi	−2 −49 13	55	Posterior cingulate

TLE-HS, temporal lobe epilepsy with hippocampal sclerosis; TLE-NL, non-lesional temporal lobe epilepsy; FLE-FCD, frontal lobe epilepsy with focal cortical dysplasia; Ipsi, ipsilateral to the syndrome lateralization; Contra, contralateral to the syndrome lateralization.

hemispheres are also affected in TLE-HS, the most significant damage is observed in the tracts directly connected with the hippocampus ipsilateral to the epileptogenic zone. The diffuse abnormal FA and RD (and the absence of AD abnormalities) observed in these patients suggest that HS pathology coexists with widespread myelin degeneration, or maldevelopment, affecting the structural connectivity of the hippocampus.[4–7,23–28]

In the present study, with the defined statistical parameters and thresholds, no micro- or macrostructural WM abnormalities were observed in the TLE-NL group. However, caution should be taken with this result and we certainly cannot affirm that TLE-NL patients have no abnormal tracts. Indeed, a previous study showed significant FA reduction on the posterior part of the cingulum on TLE-NL, suggesting that subtle abnormalities may be diluted by the whole tract analysis.[11] What is clear with our results, however, is that, if present, the WM abnormalities on TLE-NL patients are subtler than what is observed for both TLE-HS and FLE-FCD. The rationale for this finding could be the different substrate of underlying pathology in TLE-NL or the significant older age of epilepsy when most of the WM maturation has occurred. This hypothesis is supported by a previous study showing that FA increases with age for most of the tracts, more rapidly initially in early ages and reaching a plateau during the late teens or twenties.[22]

In the FLE-FCD group, FA abnormalities were seen only in the BoC, which is the fasciculus anatomically related to the frontal region. The IFO fasciculi are also related to the frontal regions but possible alterations in the frontal portion of this tract (which is a small portion of the whole tract) could be diluted. In addition, RD abnormalities were found

only in the cingulum of FLE-FCD patients. The VBM analysis of the FLE-FCD group showed WM atrophy in areas concordant to the DTI study, including areas ipsilateral to the epileptogenic zone, such as posterior cingulate and medial frontal gyrus. In contrast to the TLE-NL group, the FLE-FCD patients had subtle structural MRI lesions. This information agrees with the hypothesis that focal cortical lesions could widely affect the structural connectivity by a consequent net of axon degeneration.

Considering the other atrophic areas indicated by the VBM in the FLE-FCD group, it is notable the coincidence of the WM alterations with the ipsilateral structures of the default mode network (DMN).[29] The DMN concept is based on a set of brain areas that consistently activates in passive control situations and that could be accessed during resting state functional MRI experiments. DMN could be associated with spontaneous cognition, as recounting of recent happenings and expectations about the future.[30] Furthermore, in the DTI analysis, the only abnormal tract detected in FLE-FCD was the ipsilateral cingulum, which connects the posterior cingulate cortex to the medial frontal cortex, two important components of the DMN.[31] Decreased connectivity in areas of the DMN ipsilateral to the epileptogenic zone has been detected in patients with FLE-FCD.[32] This pattern of WM disruption was not observed in the two TLE groups. Although in the TLE-HS group the BoC was also abnormal in the DTI analysis, the VBM analysis demonstrated WM damage only to the anterior portion of the cingulum, which is indeed connected to the limbic system.[32]

We have demonstrated the distinct patterns of WM damage in patients with different AED-resistant epilepsy syndromes; however, we certainly cannot definitely answer what are the determinants of the occurrence of this injury. One possible mechanism associated with the WM damage is the occurrence of seizures and the pattern of seizure propagation. In this study, all patients were refractory to AEDs. Because this is a cross-sectional study, the number of seizures across life could not be specifically determined. However, we could compare the occurrence or not of secondary generalized tonic–clonic seizures (SGTCS) in the year prior to the MRI acquisition. As expected for clinical cohorts of patients with epilepsy, the group with the lower number of individuals with SGTCS was the TLE-HS group. However, this is exactly the group with the most significant WM abnormalities on both DTI and VBM analysis. Another possible mechanism not thoroughly evaluated so far is the influence of the underlying cause of the epilepsy in the diffuse brain structure damage. TLE-HS is the most studied form of epilepsy and, as observed in our study, this is the epileptic syndrome with the most extensive gray matter and WM injury.[2] Our study adds the information that patients with subtle MRI signs of FCD also have WM damage, while in those with normal MRI, no significant WM abnormality could be detected. This suggests that the underlying cause of the epilepsy is an important factor that could explain the abnormal WM integrity in patients with focal epilepsy. One limitation of our study is the absence of histologic confirmation of HS and FCD for all patients. We have, however, strong neuroimaging evidence that supports the classification of our patients in the three distinct groups. The definition of HS included both visual analysis and MRI quantification measurements, confirming decreased volume and hyperintense T_2 signal in the hippocampus. For patients with FLE-FCD and TLE-NL, an expert in the field (FC) performed an exhaustive MRI analysis with multiplanar reconstruction before the definition of signs of FCD or normal MRI. In addition, the small sample of patients submitted to surgery confirmed the classification in all cases (five confirmed HS in TLE-HS, two confirmed FCD in FLE-FCD, and one absence of specific histology findings in TLE-NL). In addition, one may argue that this could be a limitation to accurately define the lateralization of the epileptogenic zone masking some abnormalities, especially in the group with normal tracts, TLE-NL. However, the patients included in the present study have undergone a strict selection and only those with clear lateralization of the epileptogenic zone were selected, as described in the methods.

The lateralization of the MRI scans according to the epileptogenic zone in the present study enabled the observation of specific abnormalities of each epilepsy type using a larger number of subjects. However, this methodology does not allow inferences about brain hemispheres particularities. It is known that the epileptogenic hemisphere includes more relevant WM alterations, but previous DTI studies have also shown differences between right and left TLE patients.[10] The aim of the present study was to compare epilepsy-specific abnormalities, regardless of side of epileptogenic zone, and side-specific subanalysis should be done in the future with a larger sample size.

As described earlier, another limitation is the absence of the segmental analysis of the selected tracts. This approach could increase the sensitivity to detect abnormalities, especially in the group of patients with TLE-NL, and we believe it has its most importance in the analysis of patient-specific abnormalities, what was not the aim of the present study. In fact, the statistical approach applied in this study most likely detected abnormalities present in most patients in each group, while it likely missed additional WM abnormalities present in individual patients.

In conclusion, WM integrity is disrupted in AED-resistant localization-related epilepsies, and this abnormality varies according to the underlying pathologic substrate and localization of seizure focus. Although the implications of these WM abnormalities remain unknown, further studies with larger sample size may help to characterize specific focal WM disruptions associated with epileptogenic lesions in individual patients with localization-related epilepsies.

Whether these WM abnormalities will help in predicting response to clinical and surgical treatment remains to be determined.

Acknowledgments

Study supported by FAPESP (Fundação de Amparo á Pesquisa do Estado de São Paulo), grant 2013/07559-3. ACC was funded by FAPESP, grant 2013/00099-7.

Disclosure

None of the authors has any conflict of interest to disclose. We confirm that we have read the Journal's position on issues involved in ethical publication and affirm that this report is consistent with those guidelines.

References

1. Mueller SG, Laxer KD, Cashdollar N, et al. Voxel-based optimized morphometry (VBM) of gray and white matter in Temporal Lobe Epilepsy (TLE) with and without mesial temporal sclerosis. *Epilepsia* 2006;47:900–907.
2. Coan AC, Campos BM, Yasuda CL, et al. Frequent seizures are associated with a network of gray matter atrophy in temporal lobe epilepsy with or without hippocampal sclerosis. *PLoS ONE* 2014;9: e85843.
3. Yasuda CL, Valise C, Saúde AV, et al. Dynamic changes in white and gray matter volume are associated with outcome of surgical treatment in temporal lobe epilepsy. *NeuroImage* 2010;49:71–79.
4. Gross DW, Concha L, Beaulieu C. Extratemporal white matter abnormalities in mesial temporal lobe epilepsy demonstrated with diffusion tensor imaging. *Epilepsia* 2006;47:1360–1363.
5. Rodrigo S, Oppenheim C, Chassoux F, et al. Unicnate fasciculus fiber tracking in mesialtemporal lobe epilepsy. Initial findings. *Eur Radiol* 2007;17:1663–1668.
6. Concha L, Kim H, Bernasconi A, et al. Spatial patterns of water diffusion along white matter tracts in temporal lobe epilepsy. *Neurology* 2012;79:455–462.
7. Liacu D, Idy-Peretti I, Ducreux D, et al. Diffusion tensor imaging tractography parameters of limbic system bundles in temporal lobe epilepsy patients. *J Magn Reson Imaging* 2012;36:561–568.
8. Gross DW, Bastos A, Beaulieu C. Diffusion tensor imaging abnormalities in focal cortical dysplasia. *Can J Neurol Sci* 2005;32:477–482.
9. Duffau H, Thiebaut de Schotten M, Mandonnet E. White matter functional connectivity as an additional landmark for dominant temporal lobectomy. *J Neurol Neurosurg Psychiatry* 2008;79:492–495.
10. Ahmadi ME, Hagler DJ Jr, McDonald CR, et al. Side matters: diffusion tensor imaging tractography in left and right temporal lobe epilepsy. *AJNR* 2009;30:1740–1747.
11. Scanlon C, Mueller SG, Cheong I, et al. Grey and white matter abnormalities in temporal lobe epilepsy with and without mesial temporal sclerosis. *J Neurol* 2013;260:2320–2329.
12. Concha L, Beaulieu C, Collins DL, et al. White-matter diffusion abnormalities in temporal-lobe epilepsy with and without mesial temporal sclerosis. *J Neurol Neurosurg Psychiatry* 2009;80:312–319.
13. Liu M, Concha L, Lebel C, et al. Mesial temporal sclerosis is linked with more widespread white matter changes in temporal lobe epilepsy. *Neuroimage Clin* 2012;1:99–105.
14. Eriksson SH, Rugg-Gunn FJ, Baker GJ, et al. Diffusion tensor imaging in patients with epilepsy and malformations of cortical development. *Brain* 2001;124:617–626.
15. Diehl B, Tkachc I, Piaoa P, et al. Diffusion tensor imaging in patients with focal epilepsy due to cortical dysplasia in the temporo-occipital region: electro-clinico-pathological correlations. *Epilepsy Res* 2010;90:178–187.
16. Blümcke I, Thom M, Aronica E, et al. The clinicopathologic spectrum of focal cortical dysplasias: a consensus classification proposed by an ad hoc Task Force of the ILAE Diagnostic Methods Commission. *Epilepsia* 2011;52:158–174.
17. Coan AC, Bergo FPG, Campos BM, et al. 3T MRI quantification of hippocampal volume and signal in mesial temporal lobe epilepsy improves detection of hippocampal sclerosis. *AJNR* 2014;35:77–83.
18. Cendes F. Neuroimaging in investigation of patients with epilepsy. *Epilepsy* 2013;19:623–642.
19. Beaulieu C. The basis of anisotropic water diffusion in the nervous system - a technical review. *NMR Biomed* 2002;15:435–455.
20. Parker GJM, Wheeler-Kingshott CAM, Barker GJ. Estimating distributed anatomical connectivity using fast marching methods and diffusion tensor imaging. *IEEE Trans Med Imaging* 2002;21:505–512.
21. Gross DW. Diffusion tensor imaging in temporal lobe epilepsy. *Epilepsia* 2011;52:32–34.
22. Lebel C, Walker L, Leemans A, et al. Microstructural maturation of the human brain from childhood to adulthood. *NeuroImage* 2008;40:1044–1055.
23. Focke NK, Yogarajah M, Bonelli SB, et al. Voxel-based diffusion tensor imaging in patients with mesial temporal lobe epilepsy and hippocampal sclerosis. *NeuroImage* 2008;40:728–737.
24. Crespela A, Coubes P, Rousseta MC, et al. Inflammatory reactions in human medial temporal lobe epilepsy with hippocampal sclerosis. *Brain Res* 2002;952:159–169.
25. Milesi G, Garbelli R, Zucca I, et al. Assessment of human hippocampal developmental neuroanatomy by means of ex-vivo 7 T magnetic resonance imaging. *Int J Dev Neurosci* 2014;34:33–41.
26. Bonilha L, Tabesh A, Dabbs K, et al. Neurodevelopmental alterations of large-scale structural networks in children with new-onset epilepsy. *Hum Brain Mapp* 2014;35:3661–3672.
27. Amarreh I, Dabbs K, Jackson DC, et al. Cerebral white matter integrity in children with active versus remitted epilepsy 5 years after diagnosis. *Epilepsy Res* 2013;107:263–271.
28. Mathern GW, Adelson PD, Cahan LD, et al. Hippocampal neuron damage in human epilepsy: Meyer's hypothesis revisited. *Prog Brain Res* 2002;135:237–251.
29. Van den Heuvel M, Mandl R, Luigjes J, et al. Microstructural organization of the cingulum tract and the level of default mode functional connectivity. *J Neurosci* 2008;28:10844–10851.
30. Greicius MD, Krasnow B, Reiss AL, et al. Functional connectivity in the resting brain: a network analysis of the default mode hypothesis. *PNAS* 2003;100:253–258.
31. Widjaja E, Zamyadi M, Raybaud C, et al. Abnormal functional network connectivity among resting-state networks in children with frontal lobe epilepsy. *AJNR* 2013;34:2386–2392.
32. Concha L, Gross DW, Beaulieu C. Diffusion tensor tractography of the limbic system. *Am J Neuroradiol* 2005;26:2267–2274.

Supporting Information

Additional Supporting Information may be found in the online version of this article:

Table S1. Detailed clinical information of patients.